THE JOURNAL OF PHYSICAL CHEMISTRY C

Article

pubs.acs.org/JPCC

Enhancement of the Yield of Photoinduced Charge Separation in Zinc Porphyrin–Quantum Dot Complexes by a Bis(dithiocarbamate) Linkage

Shengye Jin,[†] Mario Tagliazucchi,[†] Ho-Jin Son,[†] Rachel D. Harris,[†] Kenneth O. Aruda,[†] David J. Weinberg,[†] Alexander B. Nepomnyashchii,[†] Omar K. Farha,[†,‡] Joseph T. Hupp,[†] and Emily A. Weiss*[,†]

[†]Department of Chemistry, Northwestern University, 2145 Sheridan Road, Evanston, Illinois 60208, United States

[‡]Department of Chemistry, Faculty of Science King Abdulaziz University, Jeddah, Saudi Arabia

Supporting Information

ABSTRACT: This paper describes the use of a phenyl bis(dithiocarbamate) (PBTC) linker to enhance the quantum yield of photoinduced electron transfer (eT) from a zinc porphyrin (ZnP) molecule (donor) to a CdSe quantum dot (QD) (acceptor), where quantum yield is defined as the fraction of photoexcited ZnP molecules in the sample that donate an electron to the QD. The PBTC ligand links the ZnP to the QD by coordinating to Cd^{2+} on the surface of the QD and the Zn metal center in ZnP via its dithiocarbamate groups. Compared with the donor–acceptor complex formed in the absence of PBTC linkers, where the ZnP molecule adsorbs to the QD through its carboxylate moiety, the PBTC linkage increases the binding affinity between ZnP molecules and QDs by an order of magnitude, from $1.0 \times 10^5 \pm (0.7 \times 10^4)$ M^{-1} to $1.0 \times 10^6 \pm (1.0 \times 10^5)$ M^{-1}, and thereby increases the eT quantum yield by, for example, a factor of 4 (from 8% to 38%) within mixtures where the molar ratio ZnP:QD = 1:1.

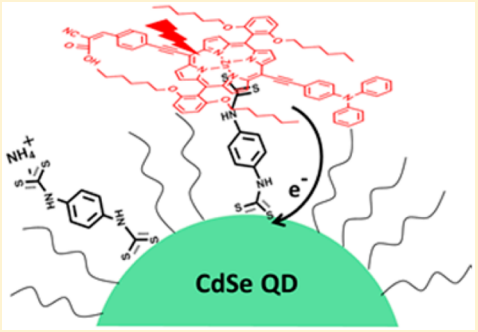

INTRODUCTION

This paper describes the enhancement of the quantum yield of electron transfer (eT) from a substituted zinc porphyrin—((2-cyano-3-*trans*-(4-(2-(10,20-bis(2,6-di(*n*-hexoxy)phenyl)-15-(*N*,*N*-diphenylbenzenamine)ethynylporphyrinato)zinc(II)-5-yl) ethynyl)phenyl)acrylic acid), here abbreviated as "ZnP"—to a CdSe quantum dot (QD) upon selective photoexcitation of the ZnP, by linking the donor–acceptor pair via a phenyl bis(dithiocarbamate) (PBTC) molecule, Figure 1A. We define quantum yield of eT as the fraction of photoexcited ZnP molecules in the sample (bound to a QD or freely diffusing) that transfer an electron to a CdSe QD rather than decaying by another radiative or nonradiative pathway. For electron transfer to quantitatively out-compete other radiative and nonradiative electron relaxation pathways within QD-molecule systems, it needs to occur on the single-picosecond to hundreds-of-picoseconds time scale.[1] The majority of previous studies of eT between colloidal QDs and molecular redox partners have demonstrated the sensitivity of eT dynamics to donor–acceptor distance, where the QD and the molecule are separated by an inorganic shell[2−5] or a molecular linker,[6−10] and energetic driving force, which is tuned by the size and material of the QD[11−17] and the redox potentials of the molecule.[16,18] We have shown in several examples that ultrafast eT across the QD-molecule interface only occurs when the molecular redox partner is in close contact with the inorganic surface of the particle—either through a covalent linkage or by permeating the native ligand shell of the QD to physisorb to its core.[19−21] An optimal linking strategy is therefore one that leads to a high binding affinity between the QD and the molecule, and thereby allows the maximal number of absorbed photons to result in charge separation. Here we show that the PBTC linker increases the affinity of the ZnP donor for the surface of the QD acceptor (relative to a carboxylate linkage).

We demonstrate that PBTC links the ZnP to the QD by coordinating to Cd^{2+} on the surface of the QD through one of its dithiocarbamate groups and coordinating to the Zn metal center in ZnP with its second dithiocarbamate group. We compare the quantum yield of eT for PBTC-linked ZnP–QD complexes to that of ZnP–QD complexes formed in the absence of PBTC (these complexes are presumably linked through the carboxylate functional group appended to the ZnP, Figure 1B). The PBTC linking chemistry increases the fraction of QDs that participate in eT with ZnP by, for example, a factor of 4 for QD/ZnP mixtures with a molar ratio ZnP:QD = 1:1 from that of samples without added PBTC by increasing the average number of ZnP molecules adsorbed per QD. The dynamics of formation of the reduced QD reveal that the eT process influences the dynamics of the donor–acceptor system on the 100 ps time scale, but the overlapping signals of the ZnP

Received: January 4, 2015
Revised: February 12, 2015
Published: February 12, 2015

DOI: 10.1021/acs.jpcc.5b00074
J. Phys. Chem. C 2015, 119, 5195−5202

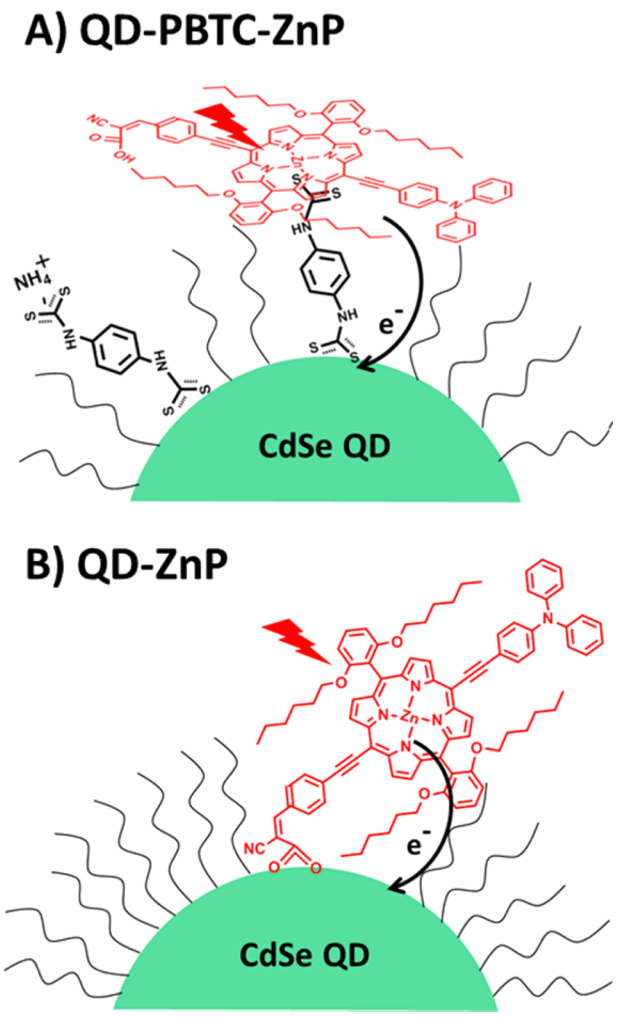

Figure 1. Most probable adsorption geometries and photoinduced eT schemes for carboxylate-functionalized ZnP molecules on CdSe QDs coated with a mixed monolayer of OPA and PBTC ligands (A) and on OPA-coated CdSe QDs (B). In part A, the ZnP molecule binds to the QD through the coordination of PBTC to the Zn metal center. In both cases, the ZnP is selectively excited at 700 nm, and subsequently transfers an electron to the QD.

and the QD in the transient absorption spectrum of the complex prevent us from precisely measuring the time constant for eT. Although it would be ideal to know the difference in the eT rate for PBTC vs carboxylate-linked complexes, the precise value of this rate does not influence the quantum yield of eT, because the decay pathway that competes with eT, the decay of the singlet excited state of ZnP (^{1}*ZnP), is dominated by intersystem crossing to the long-lived ^{3}*ZnP state (the quantum yield of fluorescence is only ~1% for ZnP), and charge separation is energetically favorable from both ^{1}*ZnP and ^{3}*ZnP. The quantum yield of eT therefore only depends on the number of photoexcited ZnP molecules that are bound to a QD within the mixture. It is this binding affinity that is enhanced by the PBTC linkage.

EXPERIMENTAL METHODS

Synthesis and Purification of QDs. We combined 90% technical grade trioctylphosphine oxide (TOPO, 7.76 g, 20.08 mmol), hexadecylamine (HDA, 7.76 g, 24.12 mmol), and cadmium stearate ($CdSt_2$, 0.448 g, 0.660 mmol) in a dry 100 mL three-neck round-bottom flask and heated the mixture, with stirring, to 150 °C for 1 h. Nitrogen flowed through one arm of the flask over the solution. This step serves to remove any water in the reaction mixture. The flask was sealed and heated to 330 °C under positive nitrogen flow. After the $CdSt_2$ completely dissolved, we rapidly injected trioctylphosphine selenide (TOPSe, 4 mL of 1 M solution in TOP, prepared and stored in a glovebox). We let the reaction run for 25 min and then let the flask cool to room temperature under ambient conditions. The QDs were precipitated in methanol and centrifuged at 3500 rpm for 5 min. We dispersed the resultant QD pellet in a minimal amount of hexanes (~10 mL), centrifuged for 5 min, and extracted the colored supernatant, which sat in the dark overnight while excess ligands precipitated. We again centrifuged the QD dispersion, separated the hexanes portion from the solid white pellet, and precipitated the QDs again by addition of acetone. We discarded the supernatant, dispersed the resulting pellet in a minimal amount of hexanes (~10 mL), and precipitated the QDs by addition of acetone a final time. The colored pellet was dispersed in ~20 mL of dichloromethane (CH_2Cl_2). The native ligand on the final QD product is n-octylphosphonate (OPA).[22,23]

Synthesis of Ammonium Phenyl Bis(dithiocarbamate) (PBTC). We combined *p*-phenylenediamine (1.73 g, 16 mmol) with NH_4OH (20 mL, 28−30%), stirred at 0 °C for approximately 20 min, added carbon disulfide (CS_2) (4 mL, 64 mmol) dropwise, and stirred the reaction mixture overnight at 0 °C. The resulting precipitate was gravity-filtered through VWR filter paper (Grade 413, qualitative). We washed the NH_4−PBTC product with hexanes and chloroform and dried it under ambient conditions to yield a light yellow powder.

Synthesis of Ammonium Phenyldithiocarbamate (PTC). We combined aniline (1.5 mL, 16 mmol) with NH_4OH (10 mL, 28−30%), stirred at 0 °C for approximately 20 min, added CS_2 (2 mL, 32 mmol) dropwise, and stirred the reaction mixture overnight at 0 °C. The resulting precipitate was gravity-filtered through VWR filter paper (Grade 413, qualitative). We washed the NH_4−PTC product with hexanes and chloroform and dried it under ambient conditions to yield a light yellow powder.

Synthesis of the Zinc Porphyrin (ZnP) Molecules. Chemicals for the synthesis of (2-cyano-3-*trans*-(4-(2-(10,20-bis(2,6-di(*n*-hexoxy)phenyl)-15-(*N*,*N*-diphenylbenzenamine)-ethynylporphyrinato)zinc(II)-5-yl)ethynyl)phenyl)acrylic acid (ZnP) were used as received from Sigma-Aldrich and Strem chemical companies. Solvents were dried following standard procedures prior to use and all chemicals were manipulated under nitrogen atmosphere. We recorded ^{1}H and ^{13}C NMR spectra of porphyrin dye on an Agilent 400-MR NMR spectrometer, and performed matrix-assisted laser desorption ionization time-of-flight (MALDI-TOF) mass spectrometry on a PE Voyager DE-Pro MALDI-TOF mass spectrometer (Bruker) in positive, reflector ionization mode, using dithranol as a matrix. The ZnP molecules were synthesized following Scheme S1 in the Supporting Information from [5,15-bis(ethynyl)-10,20-bis[2,6-di(*n*-hexoxy)phenyl]porphinato]zinc (**1**), 4-iodo-*N*,*N*-diphenylbenzenamine (**2**), and 2-cyano-3-(4-iodophenyl)acrylic acid (**3**), which were synthesized according to literature procedures.[24−27] We deoxygenated a stirring mixture of **1** (100 mg, 0.102 mmol), **2** (33.8 mg, 0.113 mmol), **3** (27.9 mg, 0.113 mmol), CuI (7 mg, 0.037 mmol), and PPh_3 (36 mg, 0.138 mmol) in 10 mL of NEt_3/toluene (1:5

DOI: 10.1021/acs.jpcc.5b00074
J. Phys. Chem. C 2015, 119, 5195−5202

v/v) for 10 min and then added $Pd_2(dba)_3$ (32 mg, 0.034 mmol) . The solution was then stirred at 40−50 °C for 12 h. We collected the crude compound after solvent evaporation and then purified it using silica-gel column chromatography (dichloromethane/methanol (95:5 v/v)) to obtain pure product (85.5 mg, 60% yield). The Supporting Information contains the NMR spectra and mass spectrometry data for this compound.

Ligand Exchange Procedures and Formation of QD−ZnP Complexes. We prepared PTC- or PBTC-coated QDs by displacing the OPA ligands on as-prepared CdSe QDs with PTC or PBTC in a solution-phase ligand exchange process. We added the appropriate mass of the NH_4PTC or NH_4PBTC solid into a 10 μM dispersion of the OPA-coated QDs in CH_2Cl_2, sonicated the mixture for 3 h, and then filtered the mixture to remove the undissolved solids.

We prepared the QD−ZnP complexes by simply mixing the QDs coated with mixed monolayers of OPA and PTC or PBTC with ZnP molecules in CH_2Cl_2 at a series of ZnP:QD molar ratios. Throughout the series of samples we present, the ZnP concentration is fixed and the QD concentration varies.

Transient Absorption Measurements. We used a commercial TA spectrometer (Helios, Ultrafast Systems) to collect the TA spectra for pump−probe delay times from 200 fs to 3200 ps and a commercial TA spectrometer (EOS, Ultrafast Systems) to collect the TA spectra for pump−probe delay times from 0.5 ns to 1 μs. Detailed descriptions of TA measurements are in the Supporting Information. The pump wavelength was 700 nm for all TA measurements (this wavelength selectively excites the ZnP, so no excitons are formed on the QDs in these experiments), and the pump power was approximately 0.4 μJ per pulse. Since the absorption spectra of the ZnP molecules shift for different ZnP:QD molar ratios, we adjusted the excitation power at 700 nm such that the expectation value of excited ZnP molecules is the same (∼0.1) for all samples.

RESULTS AND DISCUSSION

Phenyl Bis(dithiocarbamate) Ligands Link ZnP Molecules to the QDs by Coordinating to the Zn Metal Center. Figure 2 shows the ground state absorption spectra of ZnP molecules ("ZnP"), and of CdSe QDs ("QD"), in CH_2Cl_2. The spectrum of ZnP has two absorption peaks: the Soret band at 450 nm and the Q-band at 660 nm. The first excitonic absorption peak of the QDs is at 609 nm, based on which we estimate the size of the QD to be 2.5 nm in radius.[28]

We chose a ZnP molecule as the electron donor because (i) it has a high-extinction absorption feature that is spectrally isolated from the absorption spectrum of the QD, so it can be selectively excited when QDs are present, (ii) there is sufficient driving force for charge separation from both the singlet (E_S ∼ 1.8 eV, extracted from the absorption spectrum) and triplet (E_T ∼ 1.6 eV) excited states of ZnP[29−31] to the ZnP^+−QD^- radical pair (E_{RP} ∼1.0 eV, see the Supporting Information), and (iii) dithiocarbamates have a high affinity for Zn,[32] so the ZnP presents a potentially high-affinity binding site for PBTC-coated QDs. Porphyrins are attractive candidates for light harvesting within photovoltaic and photocatalytic cells due to their reducing power, high extinction coefficients across the visible spectrum, and an electronic structure that is tunable by both functionalizing the ring system and substituting different cations into the core.[27,33−38] The ZnP derivative that we use in this study, Figure 1, is particularly interesting for solar energy conversion applications because the triphenylamine moiety delocalizes the excited singlet state (compare the absorption spectrum of the ZnP molecule with that of a model compound without the triphenylamine and 2-cyano-3-(4-iodophenyl)-acrylic acid moieties, Scheme S1 in the Supporting Information), and, upon electron donation, the radical cation of the conjugated system.[29,39]

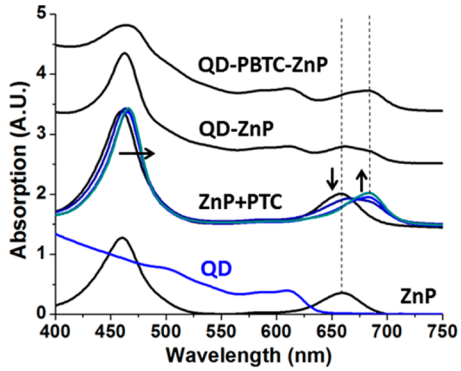

Figure 2. Ground-state absorption spectra of ZnP, OPA-coated CdSe QDs ("QD"), mixtures of ZnP and PTC with increasing amounts of PTC (from 0 mg to the amount that most ZnP molecules are coordinated) added to a 15 μM solution of ZnP ("ZnP + PTC"), a mixture of ZnP and OPA-coated CdSe QDs in a molar ratio ZnP:QD 3.3:1 ("QD−ZnP"), and a mixture of ZnP and PBTC/OPA-coated CdSe QDs in a molar ratio ZnP:QD 3.3:1 ("QD−PBTC−ZnP"), in CH_2Cl_2. The vertical dashed lines highlight the bathochromic shift of the Q-band of the ZnP molecules upon coordination of the Zn either by excess hexadecylamine in the QD−OPA−ZnP sample, by PTC in the ZnP+PTC samples, or by PBTC (and, possibly some hexadecylamine) in the QD−PBTC−ZnP sample. The arrows indicate the evolution of the spectra or kinetic traces with increasing amounts of added PTC ligands.

We examined the photoinduced eT dynamics of two different QD−ZnP complexes, differentiated by their available adsorption geometries for the ZnP on the surface of the QD. The native ligand of QDs is octylphosphonate (OPA). To prepare the first complex (which we denote "QD−ZnP", Figure 1B), we made mixtures of ZnP and OPA-coated CdSe QDs in CH_2Cl_2. Figure 2 shows the ground state absorption spectrum of this mixture ("QD−ZnP"), where the molar ratio of ZnP to QDs is 3.3:1. Comparison of this spectrum to the spectrum of free ZnP molecules (also Figure 2) shows that the Q-bands of a portion of ZnP molecules in the QD−ZnP mixture shift to lower energy by ∼20 nm. This type of shift is characteristic of coordination of the zinc metal center in ZnP with an electron donating ligand;[40,41] we believe the coordinating molecule is, in this case, hexadecylamine, which is a reagent in the synthesis of QDs and is not always completely washed out during purification. Figure S3 in the Supporting Information shows that this shifted Q-band is also present in the spectrum of mixtures of ZnP with hexadecylamine (in the absence of QDs). The most probable adsorption geometry for the QD−ZnP complex in the absence of any added linker is coordination of the carboxylate functional group of the ZnP molecules to Cd^{2+} on the surfaces of the QDs, Figure 1B, although some ZnP molecules may be physisorbed to the ligand shell of QD.

To prepare the second type of QD−ZnP complex, which we denote "QD−PBTC−ZnP", Figure 1A, we first treated the OPA-coated CdSe QDs with various amounts of the bifunctional PBTC molecules (with NH_4^+ as the counterion) by mixing in CH_2Cl_2 and sonicating for 3 h to facilitate ligand

DOI: 10.1021/acs.jpcc.5b00074
J. Phys. Chem. C 2015, 119, 5195−5202

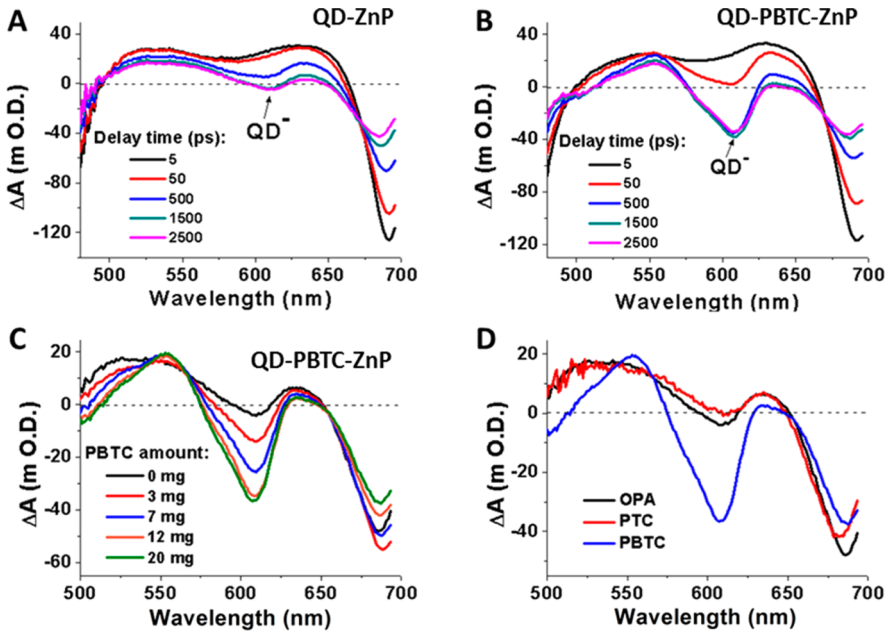

Figure 3. TA spectra acquired after 700 nm excitation of the ZnP for mixtures of ZnP and QDs under various conditions. Following the selective excitation of the ZnP molecules, a bleach of the ground state of the CdSe QDs forms at 610 nm; this bleach is due to photoinduced eT from ZnP molecules to CdSe QDs to form the QD anion. (A) TA spectra at a series of pump−probe delay times of a mixture of ZnP and OPA-coated CdSe QDs (QD−ZnP). Some QD^- forms due to binding of the ZnP to the QD through its carboxylate group and subsequent eT (Figure 1B). (B) TA spectra at a series of pump−probe delay times of a mixture of ZnP and PBTC-coated CdSe QDs (QD−PBTC−ZnP, where the QDs were treated with 20 mg PBTC). The maximum amplitude of the bleach at 610 is much more prominent in the presence of PBTC than in part A. Evolution of the ZnP bleach after 500 ps (once the eT is over) is due to unbound ZnP. (C) TA spectra at a delay time of 1500 ps for mixtures of ZnP with PBTC-coated CdSe QDs where the QDs have been treated with different amounts of PBTC ligands. The molar ratio ZnP:QD is 3.3:1 for all samples. (D) Comparison of the TA spectra at a delay time of 1500 ps (where the bleach reaches maximum amplitude) for mixtures of ZnP with PBTC-coated QDs (reproduced from panel B), mixtures of ZnP with OPA-coated QDs (reproduced from panel A), and mixtures of ZnP with PTC-coated QDs (where the QDs were treated with ∼5 mg of PTC).

exchange. The mixture was then filtered to remove the undissolved PBTC. The PBTC salt is only sparingly soluble in CH_2Cl_2, so we report the mass, rather than molarity, of PBTC we add to the QDs for each experiment. Dithiocarbamates are known chelators of Cd^{2+},[32] and we have shown previously that phenyldithiocarbamate has a high affinity for the surface of cadmium chalcogenide QDs.[42−44] We have not quantified the surface coverage of PBTC on the QDs because the NMR spectra of tightly bound ligands on QDs are too broadened to integrate accurately,[45] and because these QDs are too large to display a measurable bathochromic shift of their absorption spectra upon addition of dithiocarbamate.[42] As expected based on the limited solubility of free PBTC, the NMR spectrum of the solution of PBTC-coated QDs does not show the presence of free PBTC (see Figure S4 in the Supporting Information).

Figure 2A shows the ground state absorption spectrum of a mixture of ZnP and PBTC-coated QDs ("QD−PBTC−ZnP"), prepared by adding 20 mg of PBTC to 2 mL of 10 μM QDs, at a molar ratio ZnP:QD of 3.3:1. The ratio of intensities of the red-shifted Q-band to the unperturbed Q-band of ZnP is approximately a factor of 2 larger in the spectrum of the QD−PBTC−ZnP sample than in the spectrum of the QD−ZnP sample. The difference between these two absorption spectra is the first piece of evidence that the bifunctional PBTC linker provides an additional geometry through which the ZnP molecules adsorb to the QDs, and that this adsorption geometry, Figure 1A, involves coordination of the Zn.

In order to confirm that the absorption spectrum that we collected for the QD−PBTC−ZnP sample is indicative of coordination of PBTC ligands to ZnP molecules through the Zn, and not, for example, nonspecific interaction of ZnP with the QD, we acquired the absorption spectra of ZnP molecules in CH_2Cl_2 with various amounts of added phenyldithiocarbamate (PTC, with NH_4^+ as the counterion), which only has one dithiocarbamate group on the phenyl ring. There are no QDs in these samples. We use PTC, and not PBTC, in this control experiment because (i) PTC is more soluble in CH_2Cl_2 than is PBTC, and (ii) we do not want to form PBTC-linked dimers of ZnP, which could have additional spectral features due to ZnP−ZnP interactions. Figure 2A shows that the addition of increasing amounts of PTC to ZnP molecules (in the absence of the QDs) does, in fact, lead to a decrease in the intensity of the Soret band of uncoordinated ZnP and an increase in the intensity of the red-shifted Soret band of coordinated ZnP, the same trend we observe in the QD−PBTC−ZnP mixtures. Figure S5 in the Supporting Information shows that the PL spectra of samples of ZnP evolve similarly to the absorption spectra with increasing added amounts of PTC.

Use of PBTC to Link the ZnP Donor with the QD Acceptor Increases the Yield of Electron Transfer by Increasing the QD−ZnP Binding Affinity. We measured the yield of photoinduced eT in QD−ZnP and QD−PBTC−ZnP complexes with TA spectroscopy. Parts A and B of Figure 3 show the TA spectra for QD−ZnP (**A**) and QD−PBTC−ZnP (**B**) samples (where we prepared the PBTC-coated QDs by adding 20 mg of PBTC to 2 mL QDs of 10 μM), at a series of delay times after selective photoexcitation of ZnP molecules at 700 nm (the QDs do not absorb light at this wavelength). The molar ratios ZnP:QD are 3.3:1 for both types of samples.

DOI: 10.1021/acs.jpcc.5b00074
J. Phys. Chem. C 2015, 119, 5195−5202

The Supporting Information, Figures S6 and S7, contains the TA spectra of isolated QDs and isolated ZnP molecules that we used to assign these peaks in the spectra of the complexes. Upon excitation at 700 nm, we observe the formation of bleaches of the Q-band and Soret bands of ZnP at ~680 and 460 nm, respectively. The spectra also include a series of broad photoinduced absorptions (PIAs) between 500 and 675 nm associated with the reduced QD (QD^-, peaked at 556 nm), and corresponding to the singlet and triplet excited states of ZnP, where the oscillator strength of ^{1}*ZnP is approximately a factor of 10 larger than that of ^{3}*ZnP.[46] Parts A and B of Figure 3 show that as the photoinduced absorptions of ZnP decay, a bleach of the ground state of the QDs (centered at 610 nm) forms. We do not observe the formation of a bleach at 610 nm in the TA spectra of ZnP in the absence of QDs (see Figure S6). Bleaching of the QD ground state spectrum is a result of filling of the $1S_e$ level (LUMO) of the QD,[47] so the observed evolution of the TA spectra indicates that eT is occurring from the LUMO of ZnP to the LUMO of the QD to form QD^-. The presence of the QD bleach without excitation of the QDs is conclusive evidence of electron transfer; neither energy transfer nor hole transfer is possible in this system given the relative bandgaps and the energies of the frontier orbitals of the QD and ZnP (see the Supporting Information, Figure S2). Furthermore, we did not observe any two-photon absorption by the QDs at the excitation wavelength of 700 nm and the power of 0.4 μJ per pulse.

Electron transfer from ZnP molecules to QDs occurs in both QD−ZnP (Figure 3A) and QD−PBTC−ZnP (Figure 3B) samples, but the maximum bleach signal at 610 nm for QD−PBTC−ZnP complex is clearly more prominent than that for the QD−ZnP complex. Since the QD:ZnP molar ratio and the average number of ZnP molecules excited are the same for both samples, the enhanced magnitude of the ground state bleach signal indicates that more QDs are reduced by ZnP within samples of QD−PBTC−ZnP complexes than within samples of QD−ZnP complexes.[48] This result suggests that the functionalization of the QDs with PBTC linkers increases the number of ZnP molecules and QDs that are bound in eT-active geometries. As we asserted previously, the absorption and fluorescence spectra of QD−PBTC−ZnP are characteristic of ZnP with coordinated Zn, and indicate that this eT-active geometry is that shown in Figure 1A.

Figure 3C shows the TA spectra, at 1500 ps after selective excitation of ZnP at 700 nm, for a set of QD−PBTC−ZnP samples where the QDs have various surface coverages of PBTC. We achieve these different surface coverages by treating the QDs with different amounts of PBTC during the ligand exchange, as noted in the legend. All five samples have a molar ratio ZnP:QD of 3.3:1. The maximum magnitude of the QD ground state bleach increases as the surface coverage of the PBTC increases; the trend appears to saturate between 12 and 20 mg added PBTC. We therefore conclude that ZnP has a higher binding affinity for PBTC-coated QDs than for OPA-coated QDs.

To verify that the binding geometry of ZnP molecules on PBTC-coated QDs is, in fact, through coordination of Zn by the second dithiocarbamate group, we prepared QDs coated with PTC, rather than PBTC, by sonicating the QDs (2 mL, 10 μM) with ~5 mg PTC for 3 h. PTC binds to the QD through its dithiocarbamate group, but, unlike PBTC, it does not have available a second dithiocarbamate group to bind to the ZnP. Also unlike PBTC, addition of more than 5 mg of PTC to the QDs causes the QDs to precipitate because the solubility of these ligands in CH_2Cl_2 allows them to efficiently displace solubilizing OPA ligands. Figure 3D shows the comparison of TA spectra for (i) QD−ZnP (presumably linked through the carboxylate, Figure 1B), (ii) a mixture of ZnP with PBTC-coated QDs (where QDs were treated by 20 mg PBTC), and (iii) a mixture of ZnP with PTC-coated QDs, all at a delay time of 1500 ps, when the QD bleach reaches its maximum value. The ZnP:QD molar ratio is 3.3:1 for all these samples. The amplitude of the QD bleach signal in the spectrum of QD−PTC−ZnP complex is similar to that in the spectrum of QD−ZnP; both are four times smaller than that in the spectrum of QD−PBTC−ZnP. This result supports the binding geometry that we propose in Figure 1A, and indicates that the bifunctional PBTC ligand is the key to increasing the fraction of QDs that participate in the eT process.

We estimate the equilibrium adsorption constants, K_a, for complexes of the QDs and ZnP with and without the PBTC linker from the dependence of the magnitude of the QD bleach signal on the molar ratio ZnP:QD within a series of samples of these complexes, with molar ratios ZnP:QD between 1:1 and 1:8. We fit these data with the expression for K_a given by eq 1, where ΔA_{QD} is the magnitude of the fully formed QD bleach signal

$$K_a = \frac{m\Delta A_{QD}}{[\mathrm{QD}]_0(QY_{eT,int}[\mathrm{ZnP}]_0 - m\Delta A_{QD})} \quad (1)$$

after eT, m is the magnitude of the bleach due to reduction of one QD in the sample (the "extinction coefficient" of QD^-), $[QD]_0$ and $[ZnP]_0$ are the concentrations of QDs and ZnP molecules, respectively, added to the mixture, and $Q_{YeT,int}$ is the intrinsic quantum yield of eT for a bound QD−ZnP pair, the number of charge separated states produced per photoexcited ZnP molecule within a QD−ZnP complex. This intrinsic yield is always ~1, because, regardless of binding geometry, both ^{1}*ZnP and ^{3}*ZnP have enough energy to undergo charge separation to QD^-−ZnP^+ (see refs 29 and 30 and the Supporting Information), which, as we describe below, occurs in less than 1 ns. The vast majority of ^{1}*ZnP states will therefore decay by eT or by ISC (since fluorescence occurs on the nanosecond time scale), and the vast majority of ^{3}*ZnP states will decay by eT (since phosphorescence occurs on the microsecond time scale). We present a detailed derivation of eq 1 in the Supporting Information.

Figure S8 in the Supporting Information shows a plot of the QD ground state bleach signal as a function of $[QD]_0$ and corresponding QD:ZnP molar ratio for a series of QD−PBTC−ZnP and QD−ZnP complexes. Fit of these data by eq 1 yields adsorption constants of $K_a = 1.0 \times 10^6 \pm (1.1 \times 10^5)$ M^{-1} for QD−PBTC−ZnP (where the QDs have been treated with 20 mg PBTC) and $K_a = 1.0 \times 10^5 \pm (0.7 \times 10^4)$ M^{-1} for QD−ZnP complexes, where the uncertainty originates from the quality of the fit (the noise in the magnitude of the transient absorption signal is negligible relative to the signal).

We calculate the total eT quantum yields ($QY_{eT,tot}$), the fraction of photoexcited ZnP molecules (bound or unbound) that transfer an electron to a CdSe QD rather than decaying by another radiative or nonradiative pathway, for the QD−ZnP and QD−PBTC−ZnP systems, using eq 2. For example, for QD−ZnP and QD−PBTC−ZnP (with 20 mg

DOI: 10.1021/acs.jpcc.5b00074
J. Phys. Chem. C 2015, 119, 5195−5202

$$QY_{eT,tot} = \frac{[QD{-}ZnP]}{[ZnP]_0} QY_{eT,int} \quad (2)$$

added PBTC) mixtures with a molar ratio QD:ZnP of 1:1, we use the binding constants K_a and $QY_{eT,int}$ (= 1) for the two types of complexes and eq 2 to calculate $QY_{eT,tot}$. = 38% for the QD−PBTC−ZnP complex and $QY_{eT,tot}$ = 8% for the QD−ZnP complex. The presence of bifunctional PBTC linkers increases the total eT quantum yield by a factor of 4 by enhancing the binding affinity of the QD−ZnP complex.

Estimated Dynamics of the eT Process. Figure 4 shows the dynamics of formation and partial recovery of the signal at

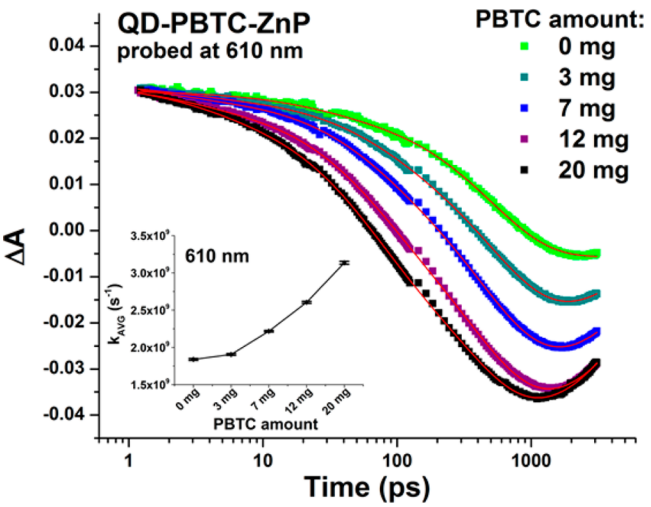

Figure 4. Kinetic traces extracted from the TA spectra of QD−ZnP and QD−PBTC−ZnP complexes (with varying surface coverages of PBTC on the QDs) at 610 nm. These traces are fit with a sum of three exponential components for the decay, and one additional exponential component for the recovery of the bleach. Inset: Intensity-averaged rate constants ($1/\tau_{AVG}$) for the decay of TA signal at 610 nm, plotted as a function of the amount of PBTC added to the QD dispersion during the ligand exchange.

610 nm, the peak of the QD ground state bleach, for the series of QD−PBTC−ZnP complexes with different surface coverage of PBTC ligands (controlled by the amount of PBTC added in the ligand exchange, between 0 and 20 mg). The main contributors to the signal at 610 nm are the QD bleach and the photoinduced absorption (PIA) of ^{1}*ZnP. All samples have a molar ratio ZnP:QD of 3.3:1. Since we do not excite the QDs directly, the bleach only forms as a result of eT. At 610 nm, we observe three time components for decay of the signal, τ_1, τ_2, and τ_3. The value of τ_1 is always approximately 2 ps, regardless of the surface coverage of PBTC on the QDs. The values of τ_2, and τ_3 depend on the surface coverage of PBTC on the QDs; see Table 1.

We know that none of these time constants is directly assignable to the eT process because, even in the absence of QDs, the excited state of the ZnP molecule decays with three time constants: τ_1 = 2.2 ps (33%), τ_2 = 37.7 ps (25%), and τ_3 = 572 ps (42%), Table 1. The triexponential nature of the excited state decay of ^{1}*ZnP (and the perturbation of the ground state absorption spectrum of this compound relative to unfunctionalized ZnP) are a result of its ethynyl linkages to diphenylbenzenamine and 2-cyano-3-(4-iodophenyl)acrylic acid moieties, and the resulting delocalization of ^{1}*ZnP, as has been seen in other ethynyl-linked ZnP complexes and ZnP-TPA complexes.[29,39,49] When not linked to these groups, the excited state of the ZnP decays with one exponential component with a time constant of ∼3 ns, corresponding to the intersystem (ISC) process (see Figure S9 in the Supporting Information). Our electrochemical measurements, which show simultaneous oxidation of ZnP and triphenylamine, and DFT calculations that show a HOMO delocalized over both components, provide strong evidence of electronic conjugation of ZnP and triphenylamine (see Figures S9 and S10 in the Supporting Information). In such large, highly conjugated systems, ultrafast dynamics are often due to vibrational reorganization and cooling of the singlet excited state,[50,51] so we assign the two faster time components τ_1 and τ_2 of ZnP (without added QDs) to this reorganization, and not to any intramolecular charge separation process. We assign τ_3 to ISC to form ^{3}*ZnP.

Upon addition of PBTC to the QDs, the intensity averaged time constant for the dynamics at 610 nm (τ_{AVG}, Table 1) decreases (see the inset to Figure 4), due mostly to a decrease in τ_3 and an increased contribution from τ_2. We interpret this result to mean that, as the fraction of ZnP molecules that participate in eT increases (which we know occurs from the increasing amplitude of the QD bleach), the dynamics of the eT process increasingly contribute to the observed dynamics on the time scale of τ_2 and τ_3 (i.e., the ∼100 ps time scale).

CONCLUSIONS

In summary, we have demonstrated that the bifunctional PBTC ligand facilitates electron transfer from photoexcited ZnP molecules to CdSe QDs within the CdSe QD−ZnP complexes by acting as a linker between Cd^{2+} on the QD surface and the Zn metal center of the porphyrin. This linkage increases the binding constant for the QD−ZnP pair by a factor of 10 over that for the pair bound by the carboxylate functionality on the porphyrin, which, in turn, increases the overall quantum yield

Table 1. Time Constants, τ (and Fractional Amplitudes, A) for Decay of the TA Signal at 610 nm (peak of the QD Bleach) for QD−ZnP and QD−PBTC−ZnP Complexes

	τ1/ps (A1)[a]	τ2/ps (A2)[a]	τ3/ps (A3)[a]	τ_{AVG} /ps[b]
ZnP only	2.2 ± 0.2 (0.330)	37.7 ± 3.0 (0.250)	571.7 ± 16.5 (0.420)	550 ± 4
ZnP−QD (no PBTC)	1.6 ± 0.5 (0.137)	47.4 ± 7.4 (0.200)	557.3 ± 14.2 (0.660)	544 ± 4
ZnP−QD with 3 mg PBTC	2.3 ± 0.3 (0.052)	63.4 ± 3.0 (0.168)	536.5 ± 11.6 (0.780)	525 ± 3
ZnP−QD with 7 mg PBTC	1.7 ± 0.2 (0.052)	58.8 ± 1.9 (0.207)	464.8 ± 5.3 (0.740)	451 ± 2
ZnP−QD with 12 mg PBTC	2.6 ± 0.3 (0.056)	56.8 ± 1.4 (0.297)	405.4 ± 5.2 (0.647)	384 ± 2
ZnP−QD with 20 mg PBTC	3.2 ± 0.3 (0.069)	51.2 ± 1.3 (0.373)	345.8 ± 5.3 (0.558)	319 ± 2

[a]Uncertainties are standard errors of the multiexponential fits of the data in Figure 4. [b]Intensity-averaged time constant: $\tau_{AVG} = (A1{\cdot}\tau_1^2 + A2{\cdot}\tau_2^2 + A3{\cdot}\tau_3^2)/(A1{\cdot}\tau_1 + A2{\cdot}\tau_2 + A3{\cdot}\tau_3)$. Uncertainties are propagated from the uncertainties of the individual time constants.

DOI: 10.1021/acs.jpcc.5b00074
J. Phys. Chem. C 2015, 119, 5195−5202

of eT (the fraction of photoexcited ZnP molecules in the sample that donate an electron to the QD) from 8% to 38% for mixtures of QDs and ZnP with a molar ratio ZnP:QD of 1:1. The eT influences the excited state dynamics of the QD−ZnP complex on the 100 ps time scale, but we cannot determine exact rate constants for eT in the various binding geometries because of overlapping signals from the ZnP and QDs over the entire visible spectrum.

Our work indicates the bifunctional PBTC and structurally similar ligands are useful for facilitating eT in both QD−co-catalyst complexes within homogeneous catalytic systems and QD−electrode or QD−metal cluster complexes in heterogeneous systems, by providing a high-affinity, geometrically well-defined linkage between the QD and its redox partner. Importantly, in systems where the QD serves as the sensitizer (as opposed to the system we have here, where the porphyrin is the sensitizer), the observed rate of eT scales linearly with the number of adsorbed electron or hole acceptors, so the effects of PBTC on eT dynamics, and not just on eT yield, will be amplified.

■ ASSOCIATED CONTENT

Ⓢ Supporting Information

Additional synthetic, experimental, and computational details, calculation of the energy of the charge-separated state, absorption, fluorescence, and transient absorption spectra of ZnP and ZnP−QD mixtures; derivation of eq 1, and cyclic voltammetry and electronic structure calculations of ZnP and model compound, including Scheme S1 and Figures S1−S11. This material is available free of charge via the Internet at http://pubs.acs.org.

■ AUTHOR INFORMATION

Corresponding Author

*(E.A.W.) E-mail: e-weiss@northwestern.edu.

Notes

The authors declare no competing financial interest.

■ ACKNOWLEDGMENTS

This work was supported by the U.S. Department of Energy, Office of Science, Basic Energy Sciences, through the Early Career Research Award (Award No. DE-SC0003998) to E.A.W. This work was also supported by the U.S. Dept. of Energy, Office of Science, Basic Energy Sciences program through a grant to J.T.H. (Award No. DE-FG87ER13808) and by Northwestern University (O.K.F.). D.J.W. is funded by the Department of Energy Office of Science Graduate fellowship program (DOE SCGF), which is administered by ORISE-ORAU under Contract Number DE-AC05-06OR23100. R.D.H. is supported by the National Science Foundation Graduate Research Fellowship Program under Grant No. DGE-1324585. The authors thank Nathaniel Swenson for calculations of orbital shapes and energies.

■ REFERENCES

(1) Knowles, K. E.; McArthur, E. A.; Weiss, E. A. A Multi-Timescale Map of Radiative and Nonradiative Decay Pathways for Excitons in CdSe Quantum Dots. *ACS Nano* **2011**, *5*, 2026−2035.

(2) Zhu, H.; Song, N.; Lian, T. Controlling Charge Separation and Recombination Rates in CdSe/ZnS Type I Core-Shell Quantum Dots by Shell Thicknesses. *J. Am. Chem. Soc.* **2010**, *132*, 15038−15045.

(3) Xu, Z. H.; Hine, C. R.; Maye, M. M.; Meng, Q. P.; Cotlet, M. Shell Thickness Dependent Photoinduced Hole Transfer in Hybrid Conjugated Polymer/Quantum Dot Nanocomposites: From Ensemble to Single Hybrid Level. *ACS Nano* **2012**, *6*, 4984−4992.

(4) Jiang, Z. J.; Kelley, D. F. Effects of Inhomogeneous Shell Thickness in the Charge Transfer Dynamics of Znte/CdSe Nanocrystals. *J. Phys. Chem. C* **2012**, *116*, 12958−12968.

(5) Sun, M. Y.; Zhu, D. H.; Ji, W. Y.; Jing, P. T.; Wang, X. Y.; Xiang, W. D.; Zhao, J. L. Exploring the Effect of Band Alignment and Surface States on Photoinduced Electron Transfer from Cuins2/CdS Core/Shell Quantum Dots to TiO2 Electrodes. *ACS Appl. Mater. Interfaces* **2013**, *5*, 12681−12688.

(6) Watson, D. F. Linker-Assisted Assembly and Interfacial Electron-Transfer Reactivity of Quantum Dot-Substrate Architectures. *J. Phys. Chem. Lett.* **2010**, *1*, 2299−2309.

(7) Kruger, S.; Hickey, S. G.; Tscharntke, S.; Eychmuller, A. Study of the Attachment of Linker Molecules and Their Effects on the Charge Carrier Transfer at Lead Sulfide Nanoparticle Sensitized ZnO Substrates. *J. Phys. Chem. C* **2011**, *115*, 13047−13055.

(8) Etgar, L.; Park, J.; Barolo, C.; Nazeeruddin, M. K.; Viscardi, G.; Graetzel, M. Design and Development of Novel Linker for PbS Quantum Dots/TiO_2 Mesoscopic Solar Cell. *ACS Appl. Mater. Interfaces* **2011**, *3*, 3264−3267.

(9) Hines, D. A.; Kamat, P. V. Quantum Dot Surface Chemistry: Ligand Effects and Electron Transfer Reactions. *J. Phys. Chem. C* **2013**, *117*, 14418−14426.

(10) Tagliazucchi, M.; Tice, D. B.; Sweeney, C. M.; Morris-Cohen, A. J.; Weiss, E. A. Ligand-Controlled Rates of Photoinduced Electron Transfer in Hybrid CdSe Nanocrystal/Poly(Viologen) Films. *ACS Nano* **2011**, *5*, 9907−9917.

(11) Jin, S. Y.; Zhang, J.; Schaller, R. D.; Rajh, T.; Wiederrecht, G. P. Ultrafast Charge Separation from Highly Reductive Znte/CdSe Type II Quantum Dots. *J. Phys. Chem. Lett.* **2012**, *3*, 2052−2058.

(12) Kongkanand, A.; Tvrdy, K.; Takechi, K.; Kuno, M.; Kamat, P. V. Quantum Dot Solar Cells. Tuning Photoresponse through Size and Shape Control of CdSe-TiO_2 Architecture. *J. Am. Chem. Soc.* **2008**, *130*, 4007−4015.

(13) Wang, D. F.; Zhao, H. G.; Wu, N. Q.; El Khakani, M. A.; Ma, D. L. Tuning the Charge-Transfer Property of PbS-Quantum Dot/TiO_2-Nanobelt Nanohybrids Via Quantum Confinement. *J. Phys. Chem. Lett.* **2010**, *1*, 1030−1035.

(14) Robel, I.; Kuno, M.; Kamat, P. V. Size-Dependent Electron Injection from Excited CdSe Quantum Dots into TiO2 Nanoparticles. *J. Am. Chem. Soc.* **2007**, *129*, 4136−4137.

(15) Zhu, H.; Song, N.; Lian, T. Wave Function Engineering for Ultrafast Charge Separation and Slow Charge Recombination in Type II Core/Shell Quantum Dots. *J. Am. Chem. Soc.* **2011**, *133*, 8762−8771.

(16) Zhu, H.; Yang, Y.; Hyeon-Deuk, K.; Califano, M.; Song, N.; Wang, Y.; Zhang, W.; Prezhdo, O. V.; Lian, T. Auger-Assisted Electron Transfer from Photoexcited Semiconductor Quantum Dots. *Nano Lett.* **2014**, *14*, 1263−1269.

(17) Yang, Y.; Rodriguez-Cordoba, W.; Lian, T. Ultrafast Charge Separation and Recombination Dynamics in Lead Sulfide Quantum Dot-Methylene Blue Complexes Probed by Electron and Hole Intraband Transitions. *J. Am. Chem. Soc.* **2011**, *133*, 9246−9249.

(18) Guchhait, A.; Pal, A. J. Correlation between Photoinduced Electron Transfer and Photovoltaic Characteristics in Solar Cells Based on Hybrid Core-Shell Nanoparticles. *J. Phys. Chem. C* **2010**, *114*, 19294−19298.

(19) Knowles, K. E.; Malicki, M.; Weiss, E. A. Dual-Time Scale Photoinduced Electron Transfer from PbS Quantum Dots to a Molecular Acceptor. *J. Am. Chem. Soc.* **2012**, *134*, 12470−12473.

(20) Malicki, M.; Knowles, K. E.; Weiss, E. A. Gating of Hole Transfer from Photoexcited PbS Quantum Dots to Aminoferrocene by the Ligand Shell of the Dots. *Chem. Commun.* **2013**, *49*, 4400−4402.

(21) Morris-Cohen, A. J.; Aruda, K. O.; Rasmussen, A. M.; Canzi, G.; Seideman, T.; Kubiak, C. P.; Weiss, E. A. Controlling the Rate of Electron Transfer between a Quantum Dot and a Tri-Ruthenium Molecular Cluster by Tuning the Chemistry of the Interface. *Phys. Chem. Chem. Phys.* **2012**, *14*, 13794−13801.

DOI: 10.1021/acs.jpcc.5b00074
J. Phys. Chem. C 2015, 119, 5195−5202

(22) Yu, W. W.; Peng, X. Formation of High-Quality CdS and Other II-VI Semiconductor Nanocrystals in Noncoordinating Solvents: Tunable Reactivity of Monomers. *Angew. Chem., Int. Ed.* **2002**, *41*, 2368−2371.
(23) Wessels, J. M.; Nothofer, H. G.; Ford, W. E.; von Wrochem, F.; Scholz, F.; Vossmeyer, T.; Schroedter, A.; Weller, H.; Yasuda, A. Optical and Electrical Properties of Three-Dimensional Interlinked Gold Nanoparticle Assemblies. *J. Am. Chem. Soc.* **2004**, *126*, 3349−3356.
(24) Splan, K. E.; Hupp, J. T. Permeable Nonaggregating Porphyrin Thin Films That Display Enhanced Photophysical Properties. *Langmuir* **2004**, *20*, 10560−10566.
(25) Lee, S. J.; Mulfort, K. L.; Zuo, X.; Goshe, A. J.; Wesson, P. J.; Nguyen, S. T.; Hupp, J. T.; Tiede, D. M. Coordinative Self-Assembly and Solution-Phase X-Ray Structural Characterization of Cavity-Tailored Porphyrin Boxes. *J. Am. Chem. Soc.* **2008**, *130*, 836−838.
(26) Wang, C. S.; Palsson, L. O.; Batsanov, A. S.; Bryce, M. R. Molecular Wires Comprising Pi-Extended Ethynyl- and Butadiynyl-2,5-Diphenyl-1,3,4-Oxadiazole Derivatives: Synthesis, Redox, Structural, and Optoelectronic Properties. *J. Am. Chem. Soc.* **2006**, *128*, 3789−3799.
(27) Lee, C. Y.; She, C. X.; Jeong, N. C.; Hupp, J. T. Porphyrin Sensitized Solar Cells: TiO_2 Sensitization with a Pi-Extended Porphyrin Possessing Two Anchoring Groups. *Chem. Commun.* **2010**, *46*, 6090−6092.
(28) Yu, W. W.; Qu, L.; Guo, W.; Peng, X. Experimental Determination of the Extinction Coefficient of CdTe, CdSe, and CdS Nanocrystals. *Chem. Mater.* **2003**, *15*, 2854−2860.
(29) She, C. X.; McGarrah, J. E.; Lee, S. J.; Goodman, J. L.; Nguyen, S. T.; Williams, J. A. G.; Hupp, J. T. Probing Exciton Localization/Delocalization: Transient Dc Photoconductivity Studies of Excited States of Symmetrical Porphyrin Monomers, Oligomers, and Supramolecular Assemblies. *J. Phys. Chem. A* **2009**, *113*, 8182−8186.
(30) Wróbel, D.; Lukasiewicz, J.; Boguta, A. The Importance of Non-Radiative Processes in Porphyrins and Phthalocyanines for Photocurrent Generation Study. *J. Phys. IV Fr.* **2003**, *109*, 111−121.
(31) Pineiro, M.; Carvalho, A. L.; Pereira, M. M.; Gonsalves, A. M. D. R.; Arnaut, L. G.; Formosinho, S. J. Photoacoustic Measurements of Porphyrin Triplet-State Quantum Yields and Singlet-Oxygen Efficiencies. *Chem.—Eur. J.* **1998**, *4*, 2299−2307.
(32) Karlin, K. Progress in Inorganic Chemistry *Prog. Inorg. Chem.*; John Wiley & Sons, Inc.: New York, 2005, *53*, 429−463.
(33) Li, L. L.; Diau, E. W. G. Porphyrin-Sensitized Solar Cells. *Chem. Soc. Rev.* **2013**, *42*, 291−304.
(34) Chappaz-Gillot, C.; Marek, P. L.; Blaive, B. J.; Canard, G.; Burck, J.; Garab, G.; Hahn, H.; Javorfi, T.; Kelemen, L.; Krupke, R.; et al. Anisotropic Organization and Microscopic Manipulation of Self-Assembling Synthetic Porphyrin Microrods That Mimic Chlorosomes: Bacterial Light-Harvesting Systems. *J. Am. Chem. Soc.* **2012**, *134*, 944−954.
(35) Yella, A.; Lee, H. W.; Tsao, H. N.; Yi, C. Y.; Chandiran, A. K.; Nazeeruddin, M. K.; Diau, E. W. G.; Yeh, C. Y.; Zakeeruddin, S. M.; Gratzel, M. Porphyrin-Sensitized Solar Cells with Cobalt (II/III)-Based Redox Electrolyte Exceed 12% Efficiency. *Science* **2011**, *334*, 629−634.
(36) Chang, Y. C.; Wu, H. P.; Reddy, N. M.; Lee, H. W.; Lu, H. P.; Yeh, C. Y.; Diau, E. W. G. The Influence of Electron Injection and Charge Recombination Kinetics on the Performance of Porphyrin-Sensitized Solar Cells: Effects of the 4-*tert*-Butylpyridine Additive. *Phys. Chem. Chem. Phys.* **2013**, *15*, 4651−4655.
(37) Wang, C. L.; Chang, Y. C.; Lan, C. M.; Lo, C. F.; Diau, E. W. G.; Lin, C. Y. Enhanced Light Harvesting with Pi-Conjugated Cyclic Aromatic Hydrocarbons for Porphyrin-Sensitized Solar Cells. *Energy Environ. Sci.* **2011**, *4*, 1788−1795.
(38) Son, H. J.; Jin, S.; Patwardhan, S.; Wezenberg, S. J.; Jeong, N. C.; So, M.; Wilmer, C. E.; Sarjeant, A. A.; Schatz, G. C.; Snurr, R. Q.; et al. J. T. Light-Harvesting and Ultrafast Energy Migration in Porphyrin-Based Metal-Organic Frameworks. *J. Am. Chem. Soc.* **2013**, *135*, 862−869.
(39) El-Khouly, M. E.; Ryu, J. B.; Kay, K.-Y.; Ito, O.; Fukuzumi, S. Long-Lived Charge Separation in a Dyad of Closely-Linked Subphthalocyanine-Zinc Porphyrin Bearing Multiple Triphenylamines. *J. Phys. Chem. C* **2009**, *113*, 15444−15453.
(40) Taylor, P. N.; Anderson, H. L. Cooperative Self-Assembly of Double-Strand Conjugated Porphyrin Ladders. *J. Am. Chem. Soc.* **1999**, *121*, 11538−11545.
(41) Anderson, H. L. Conjugated Porphyrin Ladders. *Inorg. Chem.* **1994**, *33*, 972−981.
(42) Frederick, M. T.; Amin, V. A.; Cass, L. C.; Weiss, E. A. A Molecule to Detect and Perturb the Confinement of Charge Carriers in Quantum Dots. *Nano Lett.* **2011**, *11*, 5455−5460.
(43) Frederick, M. T.; Weiss, E. A. Relaxation of Exciton Confinement in CdSe Quantum Dots by Modification with a Conjugated Dithiocarbamate Ligand. *ACS Nano* **2010**, *4*, 3195−3200.
(44) Frederick, M. T.; Amin, V. A.; Swenson, N. K.; Ho, A. Y.; Weiss, E. A. Control of Exciton Confinement in Quantum Dot-Organic Complexes through Energetic Alignment of Interfacial Orbitals. *Nano Lett.* **2013**, *13*, 287−292.
(45) Hens, Z.; Martins, J. C. A Solution NMR Toolbox for Characterizing the Surface Chemistry of Colloidal Nanocrystals. *Chem. Mater.* **2013**, *25*, 1211−1221.
(46) Huss, A. S.; Bierbaum, A.; Chitta, R.; Ceckanowicz, D. J.; Mann, K. R.; Gladfelter, W. L.; Blank, D. A. Tuning Electron Transfer Rates Via Systematic Shifts in the Acceptor State Density Using Size-Selected ZnO Colloids. *J. Am. Chem. Soc.* **2010**, *132*, 13963−13965.
(47) Klimov, V. I. Spectral and Dynamical Properties of Multiexcitons in Semiconductor Nanocrystals. *Annu. Rev. Phys. Chem.* **2007**, *58*, 635−673.
(48) Wehrenberg, B. L.; Wang, C. J.; Guyot-Sionnest, P. Interband and Intraband Optical Studies of PbSe Colloidal Quantum Dots. *J. Phys. Chem. B* **2002**, *106*, 10634−10640.
(49) D'Souza, F.; Gadde, S.; Islam, D.-M. S.; Wijesinghe, C. A.; Schumacher, A. L.; Zandler, M. E.; Araki, Y.; Ito, O. Multi-Triphenylamine-Substituted Porphyrin-Fullerene Conjugates as Charge Stabilizing "Antenna-Reaction Center" Mimics. *J. Phys. Chem. A* **2007**, *111*, 8552−8560.
(50) Chang, M.-H.; Hoffmann, M.; Anderson, H. L.; Herz, L. M. Dynamics of Excited-State Conformational Relaxation and Electronic Delocalization in Conjugated Porphyrin Oligomers. *J. Am. Chem. Soc.* **2008**, *130*, 10171−10178.
(51) Villamaina, D.; Kelson, M. M. A.; Bhosale, S. V.; Vauthey, E. Excitation Wavelength Dependence of the Charge Separation Pathways in Tetraporphyrin-Naphthalene Diimide Pentads. *Phys. Chem. Chem. Phys.* **2014**, *16*, 5188−5200.

DOI: 10.1021/acs.jpcc.5b00074
J. Phys. Chem. C 2015, 119, 5195−5202